Computational and experimental exploration of the gas-phase chemistry of alkyloxalate ions ROCOCOO– (R=H, CH3, C2H5, i-C3H7, and t-C4H9)

Héloïse Soldi-Lose, Detlef Schröder, Helmut Schwarz

Computational and experimental exploration of the gas-phase chemistry of alkyloxalate ions ROCOCOO$^-$ (R = H, CH_3, C_2H_5, *i*-C_3H_7, and *t*-C_4H_9)

Héloïse Soldi-Lose,[a] Detlef Schröder,[b] and Helmut Schwarz[a,*]

[a] *Institut für Chemie der Technischen Universität Berlin, Straße des 17. Juni 135, 10623 Berlin, Germany*

[b] *Institute of Organic Chemistry and Biochemistry, Academy of Sciences of the Czech Republic, Flemingovo nám. 2, 16610 Prague 6, Czech Republic*

Abstract:

Alkyloxalate ions ROCOCOO$^-$ (R = H, CH_3, C_2H_5, *i*-C_3H_7, and *t*-C_4H_9) are investigated by experiment and theory. Computational studies at the MP2/6-311++G(3df,3pd)//MP2/6-311++G(d) level of theory show that the structures vary with changing the size of the alkyl substituent R. Metastable ion and collisional activation mass spectra reveal three decomposition pathways of alkyloxalate ions corresponding to losses of CO and CO_2 as well as a combined expulsion of CO and CO_2. Decarbonylation dominates the spectra by far and leads to the corresponding alkylcarbonate ions ROCOO$^-$. Two mechanisms are envisaged to understand this dissociation, and calculations suggest that the reaction proceeds through the formation of an intermediate ion-neutral complex.

Keywords: ab-initio calculations, alkyloxalates, carbon oxides, decarbonylation, mass spectrometry

1. Introduction

The unimolecular reactivity of gaseous organic anions is much less often investigated compared to cations because anionic species are more difficult to generate and frequently do not show interesting decomposition features, as for example rearrangements [1]. Nevertheless, knowledge of the gas-phase behavior of such species can provide useful information for the understanding of reactions occurring in unusual environments, as for instance, in the higher terrestrial atmospheres or in the atmospheres of other planets and moons. In a project dealing with organic compounds of potential interest with respect to the atmosphere of Mars, we have

* Corresponding author: fax: + 49-30-31421102; E-Mail: Helmut.Schwarz@mail.chem.tu-berlin.de

inter alia focused our attention to a series of alkyloxalate ions (Scheme 1), which are derived from carbon dioxide, the major component of the martian atmosphere. Quite surprisingly, only very little is known about the structures as well as about the dissociation of metastable oxalate ions in the gas phase. Accordingly, here we present a systematic study of the structures and of the dissociation behavior of some representative alkyloxalate ions.

R	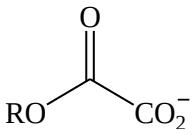
1	H
2	CH_3
3	C_2H_5
4	*i*-C_3H_7
5	*t*-C_4H_9

Scheme 1: Alkyloxalate ions investigated in this work.

Theory and experiment have been combined to probe and understand the unimolecular dissociations of the anions whose structural minima have been determined by ab initio methods. Hence, alkyloxalate ions have been generated by negative ion chemical ionization (NICI) and the mass-selected ions have been submitted to metastable ion (MI) and collisional activation (CA) experiments. Because monoalkyloxalates possess several internal rotors, these anions may exist in different conformational structures, and the structures and energetics of different conformers have been determined at the MP2/6-311++G(3df,3pd)//MP2/6-311++G(d) level of theory as well as those of the transition structures involved in the course of decomposition of the anions.

2. Experimental and computational details

The experiments were carried out with a modified VG ZAB/HF/AMD 604 four sector mass spectrometer of BEBE configuration (B stands for magnetic and E for electric sector) which has been described previously [2]. Monoalkyloxalate anions were obtained from the corresponding dialkyloxylates which are commercially available. Ca. 3 μL of the precursor were introduced to a chemical ionization (CI) source [3] in the presence of an excess of N_2O serving as a reagent gas and ionized by electrons having a kinetic energy of 100 eV at a repeller voltage of about 0 V. Due to the excess of N_2O, the formation of alkyloxalate ions

from the corresponding dialkyloxalates is likely to involve the reaction $N_2O + e^- \rightarrow N_2 + O^{\bullet -}$ as a first step, followed by a formal S_N2 reaction with the ester, $ROOCCOOR + O^{\bullet -} \rightarrow ROOCCOO^- + RO^{\bullet}$ (see Ref. [4] and references therein, and Ref. [5]); for bulky substituents R, also E2 eliminations are likely to be involved in the ion formation.

After acceleration to 8 keV kinetic energy, the ions were mass-selected with B(1). Unimolecular fragmentations of metastable ions (MI) occurring in the field-free region (ffr) preceding E1 were recorded by scanning this sector, as well as dissociation of collisionally activated ions (CA) for which a collision cell located in the ffr before E1 was filled with helium (80 % transmission, T). The data given below are averages of at least three independent measurements.

In the theoretical studies, the geometry optimizations were carried out with the MP2 method [6] using 6-311++G(d) [7,8] basis sets within the GAUSSIAN 03 suite of programs [9]. Stationary points were characterized as minima (no imaginary frequencies) or as transition structures (one imaginary frequency). The calculated frequencies were also used to determine zero point vibrational energies. Those are required for the zero-point corrections of the electronic energies and were scaled by an uniform factor of 0.9496 [10]. Refined energies were then obtained for the optimized geometries in single-point calculations employing the MP2 method in conjunction with 6-311++G(3df,3pd) basis sets [8,11].

3. Results and discussion

3.1 Structures of alkyloxalates

The structure of oxalic acid already has formed the subject of many investigations, particularly because it is one of the simplest examples of a molecule possessing three internal rotors [12-17]. It can indeed exhibit internal rotation around the central carbon-carbon bond connecting the two carbonyl groups and around the two C-OH bonds. In contrast, the structures of deprotonated oxalic acid, i.e. the hydrogen oxalate anion **1**, as well as the monoalkyloxalates $ROCOCOO^-$ have been investigated in much less detail. These anions may potentially also exist in different conformations and the determination of the conformational minimum is not obvious as will be shown below. Hence, we have investigated the different conformational structures of alkyloxalates $ROCOCOO^-$ for R = H, CH_3, C_2H_5, *i*-C_3H_7, and *t*-C_4H_9. The four conformers which correspond to the limits of the two relevant dihedral angles are presented in Scheme 2. Here, the symbols *C* and *T* refer to the conformation of the dihedral angle $O_{(1)}C_{(1)}C_{(2)}O_{(4)}$, whereas the conformers involving rotations of the $C_{(2)}$–$O_{(4)}$ bond (i.e. the dihedral angle $O_{(3)}C_{(2)}O_{(4)}R$) are denoted by *c* and *t*

(here, *c* and *C* stand for cis, *t* and *T* for trans respectively) [14]. The most relevant features of the optimized geometries of the alkyloxalates **1** to **5** in these four conformations are given in Table 1.

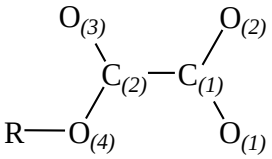

tC

$O_{(1)}C_{(1)}C_{(2)}O_{(4)}$ = 0 °

$O_{(3)}C_{(2)}O_{(4)}R$ = 0 °

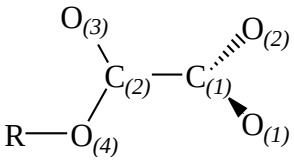

tT

$O_{(1)}C_{(1)}C_{(2)}O_{(4)}$ = 90 °

$O_{(3)}C_{(2)}O_{(4)}R$ = 0 °

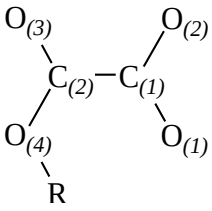

cC

$O_{(1)}C_{(1)}C_{(2)}O_{(4)}$ = 0 °

$O_{(3)}C_{(2)}O_{(4)}R$ = 180 °

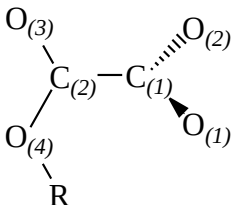

cT

$O_{(1)}C_{(1)}C_{(2)}O_{(4)}$ = 90 °

$O_{(3)}C_{(2)}O_{(4)}R$ = 180 °

Scheme 2: The four conformations of alkyloxalates anions $ROCOCOO^-$ (R = H, CH_3, C_2H_5, *i*-C_3H_7, and *t*-C_4H_9) for limiting values of the dihedral angles $O_{(1)}C_{(1)}C_{(2)}O_{(4)}$ and $O_{(3)}C_{(2)}O_{(4)}R$.

Table 1

Selected bond lengths (in Å) and bond angles (in degree) of the alkyloxalates **1** to **5** in the four conformations investigated in MP2/6-311++G(d) calculations.

		$C_{(1)}O_{(1)}$	$C_{(1)}O_{(2)}$	$C_{(1)}C_{(2)}$	$C_{(2)}O_{(3)}$	$C_{(2)}O_{(4)}$	$O_{(4)}R$	$O_{(1)}C_{(1)}O_{(2)}$	$O_{(3)}C_{(2)}O_{(4)}$
1	*tT*	1.252	1.252	1.541	1.219	1.372	0.970	132.4	120.0
	cT	1.255	1.255	1.546	1.210	1.384	0.966	128.3	118.8
	cC	1.273	1.238	1.584	1.212	1.355	0.988	127.3	122.1
	tC	1.250	1.249	1.584	1.218	1.370	0.969	132.4	119.5
2	*tT*	1.253	1.253	1.540	1.218	1.373	1.424	132.2	121.1
	cT	1.255	1.253	1.546	1.213	1.380	1.431	131.7	117.7
	cC	1.257	1.243	1.597	1.212	1.380	1.430	131.4	115.4
	tC	1.251	1.250	1.584	1.217	1.370	1.422	132.1	120.6
3	*tT*	1.254	1.253	1.540	1.218	1.375	1.430	132.2	121.6
	cT	1.256	1.253	1.545	1.213	1.381	1.436	132.1	117.7
	cC	1.257	1.243	1.598	1.212	1.382	1.435	131.4	115.5
	tC	1.251	1.250	1.584	1.217	1.372	1.426	132.1	120.7
4	*tT*	1.254	1.254	1.540	1.219	1.372	1.441	132.1	122.5
	cT	1.257	1.251	1.546	1.215	1.381	1.446	131.2	116.4
	cC	1.256	1.244	1.593	1.211	1.390	1.444	131.3	116.1
	tC	1.251	1.250	1.586	1.217	1.369	1.439	132.0	121.9
5	*tT*	1.254	1.254	1.541	1.218	1.373	1.448	132.2	122.9
	cT	1.251	1.251	1.546	1.214	1.384	1.453	131.2	116.1
	cC	1.251	1.244	1.594	1.214	1.384	1.453	131.2	116.1
	tC	1.254	1.250	1.588	1.218	1.373	1.448	132.2	122.9

The analysis of the optimized structural parameters presented in Table 1 reveals changes of bond lengths and angles of alkyloxalates between the various conformations. Rotation around the central $C_{(1)}C_{(2)}$ bond (conformers *C* and *T*) induces a minor decrease of the $C_{(1)}O_{(2)}$ bond length when passing from the *T* to the *C* conformation. This difference is moderate for the small substituents R (ca. 0.010 Å for R = H and ca. 0.007 Å for R = CH_3) and decreases even further for larger ones (ca. 0.005 Å for R = C_2H_5, *i*-C_3H_7, and *t*-C_4H_9). In marked contrast, much more pronounced changes occur for the $C_{(1)}C_{(2)}$ bond length, for which a

passage from the *T* to the *C* conformation leads to bond elongations of about 0.045 Å. This increase may be explained by steric constraints due to the "planar" backbone structure of the *C* conformation. The same reasoning also explains the difference of the $O_{(4)}$-R bond lengths observed between the *cT* and *tT* conformers and between the *cC* and *tC* structures with an average elongation of 0.005 Å in the *c* conformers. The R groups of these conformers present indeed some proximity to the carbonyl group $O_{(1)}C_{(1)}O_{(2)}$, which may hinder it to be favorably positioned for small $O_{(4)}$-R bond lengths. An elongation of the $O_{(4)}$-R bond is accordingly observed to allow a good spatial organization of the R group. For another reason, this increase is particularly important for the hydrogen oxalate ion when passing from the *tC* to the *cC* conformation (+ 0.019 Å). This latter conformation is indeed strongly stabilized through an intramolecular hydrogen bond (see below) what implies a rapprochement of the hydrogen to the $O_{(1)}$ atom. Further, as for the $O_{(4)}$R bond, a slight increase of the $C_{(1)}O_{(1)}$ bond length is observed when changing from the *t* to the *c* conformation. The $C_{(2)}O_{(3)}$ and $C_{(2)}O_{(4)}$ distances are also influenced by a rotation around the $C_{(2)}O_{(4)}$ axis. Again, both bonds are slightly longer in the *c* than in the *t* conformation. Concerning the angles, one notices that the $O_{(1)}C_{(1)}O_{(2)}$ angle remains almost unchanged for the various conformers, except for the hydrogen oxalate ion which presents a structure more "opened" by ca 4 ° in the *c* conformation compared to the *t* one. Slightly larger changes are observed for the $O_{(3)}C_{(2)}O_{(4)}$ angle which decreases by ca. 6 ° when passing from the *t* to the *c* configuration. To summarize, if one roughly compares the different conformational structures predicted by theory, it can be seen that if the central backbone is planar (*C*), the structures of alkyloxalates are elongated along the $C_{(1)}C_{(2)}$ axis. The most compact structure corresponds to the *cT* conformation and the loosest one to the *tT* conformation.

The total electronic and relative energies of alkyloxalates **1** to **5** calculated at the MP2/6-311++G(3df,3pd) level of theory for the four optimized conformational structures are given in Table 2. The number of imaginary frequencies is also included as they allow the characterization of the conformers as minima or as transition structures.

Table 2

Total energies E_{tot},[a] relative energies E_{rel},[b] and number of imaginary frequencies of the four conformers of the alkyloxylates **1** to **5** according to MP2/6-311++G(3df,3pd)//MP2/6-311++G(d) calculations.

	Conformer	E_{tot}[a] (Hartree)	E_{rel}[b] (kcal/mol)	Number of imaginary frequencies
1	*tT*	-377.1981850	8.9	0
	cT	-377.1968332	9.8	1
	cC	-377.212433	0.0	0
	tC	-377.1930629	12.2	1
2	*tT*	-416.3727241	0.3	0
	cT	-416.3732318	0.0	0
	cC	-416.3690674	2.6	1
	tC	-416.3645157	5.5	1
3	*tT*	-455.5723569	0.5	0
	cT	-455.5731566	0.0	0
	cC	-455.5688245	2.7	1
	tC	-455.5649954	5.1	1
4	*tT*	-494.7701893	0.0	0
	cT	-494.7693479	0.5	0
	cC	-494.7596878	6.6	1
	tC	-494.765386	3.0	1
5	*tT*	-533.9737309	0.0	0
	cT	-533.9731006	0.4	0
	cC	-533.9634608	6.4	1
	tC	-533.9700754	2.3	1

[a] ZPE included and uniformly scaled (0.9496).

[b] The energy is given relative to the most stable conformer for each alkyloxalate.

A comparison of the energetics of the four conformers of the alkyloxalates **2** to **5** shows that the planar conformers *cC* and *tC* correspond to transition structures, whereas the non-planar structures *cT* and *tT* are minima. A more detailed discussion for each alkyloxalate will

be presented after the examination of the particular case of the hydrogen oxalate ion. The ion with R = H differs from the other ROCOCOO$^-$ anions studied because the conformation *cC* possesses an intramolecular hydrogen bond between two oxygen atoms (Scheme 3). The resulting overall stabilization of this structure amounts to ca. 10 kcal/mol compared to the other conformers (Table 2). Furthermore, frequency calculations characterize the *tT* conformer as a minimum and the *cT* and *tT* conformers as transition structures. The results concerning the relative energies of the conformers as well as their characterization as minima or saddle points are in complete agreement with the findings of Cheng and Shyu [18] in which the four conformations of the hydrogen oxalate ion were considered at various levels of theory.

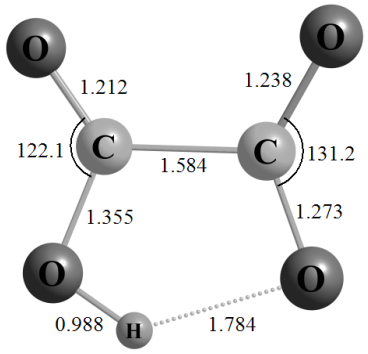

1(*cC*)

Scheme 3: Optimized structure of the most stable conformer of the hydrogen oxalate ion **1** at the MP2/6-311++G(d) level of theory.

As already mentioned, the conformations *cT* and *tC* correspond to transition structures for HOCOCOO$^-$, and the normal modes associated to the imaginary frequency of each conformer are associated with torsions around both the $C_{(1)}C_{(2)}$ and $C_{(2)}O_{(4)}$ axis. A schematic description showing the conformational connections between the relevant conformers of the hydrogen oxalate ion is presented in Figure 1.

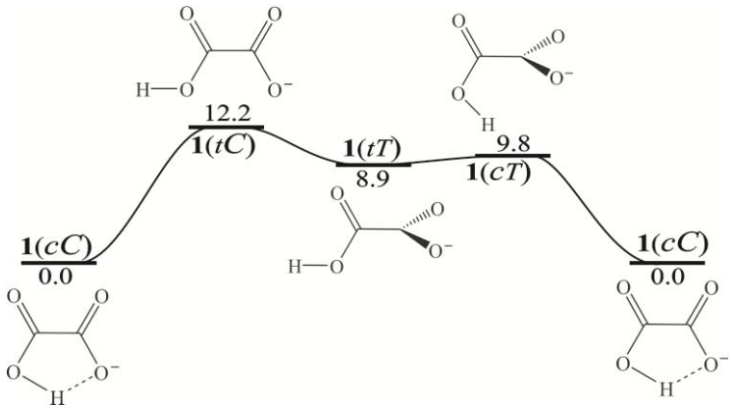

Figure 1: Connections between the different conformers of the hydrogen oxalate ion **1** according to MP2/6-311++G(3df,3pd)//MP2/6-311++G(d) calculations (energies in kcal/mol).

The conformational structures **1**(*cT*) and **1**(*tT*) differ by only 0.9 kcal/mol, and Cheng and Shyu [18] even found the transition structure **1**(*cT*) to be 0.4 kcal/mol lower in energy than the local minimum **1**(*tT*). Nevertheless, the most favorable conformer **1**(*cC*) is clearly lower in energy than all other conformational structures investigated and is accordingly assumed as the most stable conformer of the ion **1**.

Concerning the four other alkyloxalates investigated, energy calculations show that all conformers *cC* and *tC* correspond to transition structures, while the *tT* and *cT* conformers are minima. For methyl- and ethyloxalate ions, the most stable structure is the conformation *cT* whereas for *i*-propyl- and *t*-butyloxalate, it is the conformation *tT* (Figure 2).

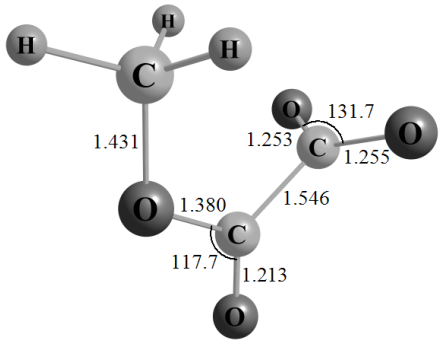

2(*cT*)

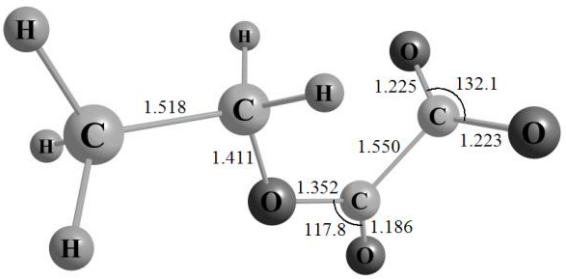

3(*cT*)

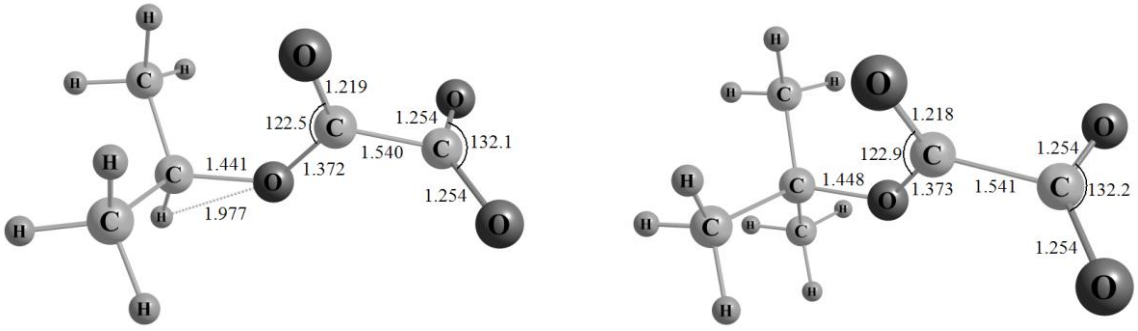

4(*tT*) **5**(*tT*)

Figure 2: The most stable conformational minima of the alkyloxalates anions **2** to **5** obtained at the MP2/6-311++G(d) level of theory.

The connections between the various conformers of the alkyloxylates **2** to **5** are not as straightforward as in the case of **1**. An analysis of the normal mode associated to the imaginary frequency of the conformers *cC* and *tC* reveals that these transition structures correspond to rotations around the $C_{(1)}C_{(2)}$ axis changing the value of the dihedral angle $O_{(1)}C_{(1)}C_{(2)}O_{(4)}$ from 0 ° to 180 °. Due to the symmetry of the carboxylate group, these two values of the dihedral angle correspond to the same conformation (Scheme 4).

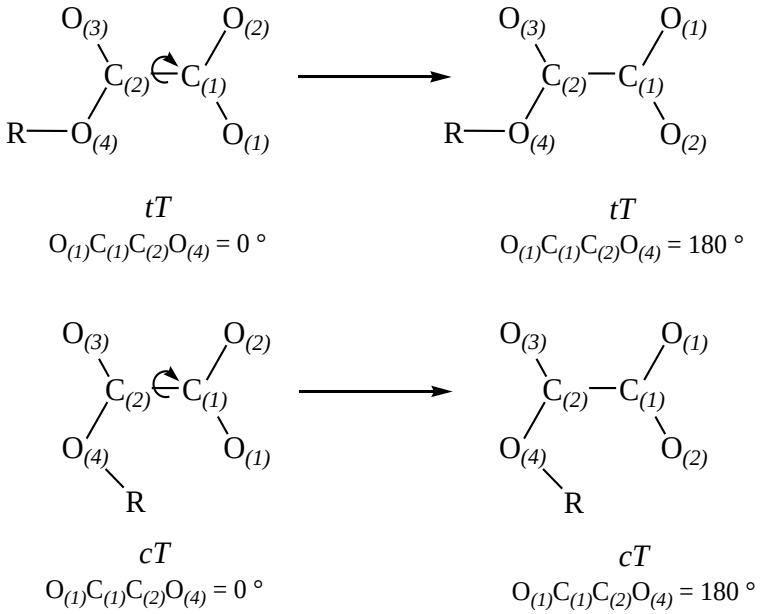

Scheme 4: The conformational structure of alkyloxalates $ROCOCOO^-$ (R = H, CH_3, C_2H_5, *i*-C_3H_7, and *t*- C_4H_9) is conserved by rotation of 180 ° around the $C_{(1)}$-$C_{(2)}$ axis due to the symmetry of the carboxylate group.

The passage of the conformation *cT* to *tT* requires a rotation around the $C_{(2)}O_{(4)}$ axis to change the dihedral angle $O_{(3)}C_{(2)}O_{(4)}R$ from 180 ° to 0 ° (R = CH_3, C_2H_5, *i*-C_3H_7, and *t*-C_4H_9). The transition structure TS(*cT*/*tT*) associated with this rotation has a T-shaped conformation and a dihedral angle $O_{(3)}C_{(2)}O_{(4)}R$ of 90 ° (R = CH_3, C_2H_5, *i*-C_3H_7, and *t*-C_4H_9). As an example, the optimized structure of the transition structure of the methyloxalate ion **2** is shown in Figure 3. The relative energies of the transition structures are given in Table 3 for the ions **2** to **5**.

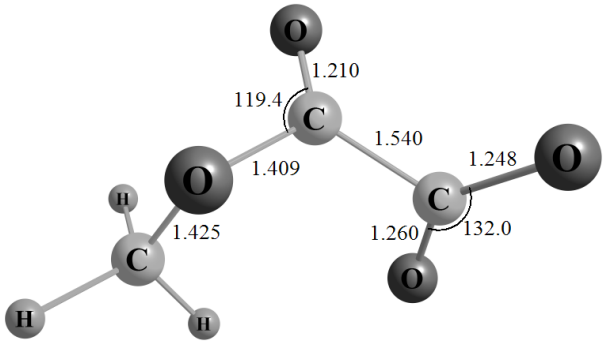

TS(*cT*/*tT*)(**2**)

Figure 3: Optimized transition structure associated to the passage of the *cT* to the *tT* conformation of methyloxalate **2** according to MP2/6-311++G(d) calculations.

Table 3

Total and relatives energies of the transition structures TS(*cT*/*tT*) for the alkyloxalates **2** to **5** according to MP2/6-311++G(3df,3pd)//MP2/6-311++G(d) level of theory.

		E_{tot} [a] (Hartree)	E_{rel} [b] (kcal/mol)
TS(*cT*/*tT*)	**2**	-416.3598209	8.4
	3	-455.5603955	8.0
	4	-494.7614792	5.5
	5	-533.9652372	5.3

[a] ZPE included and uniformly scaled (0.9496).

[b] Energies given relative to those of the corresponding alkyloxalates (Table 2) in the most stable conformation (*cT* or *tT*).

From the energetics data of the TS(*cT*/*tT*) transition structures (Table 3), a general scheme for the conformational changes of the alkyloxalates **2** to **5** can be deduced. These schemes are

presented in Figure 4a for methyl- and ethyloxalate and in Figure 4b for *i*-propyl- and *t*-butyloxalate.

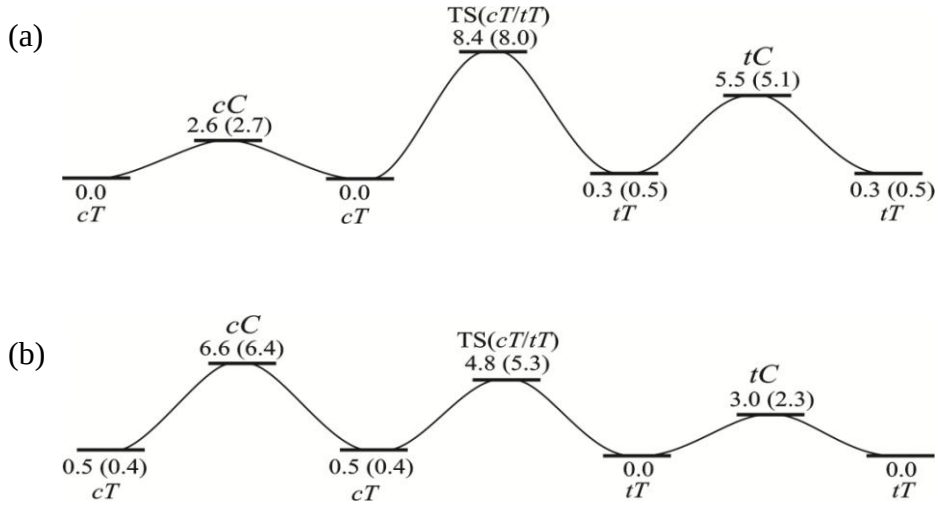

Figure 4: Conformational interconversion of (a) methyloxalate ions (data for ethyloxalate in brackets) and (b) *i*-propyloxalate ions (data for *t*-butyloxalate in brackets). Energies are given relative to the conformer (a) *cT* of methyl- and ethyloxalate and (b) *tT* of *i*-propyl- and *t*-butyloxalate according to MP2/6-311++G(3df,3pd)//MP2/6-311++G(d) calculations (energies in kcal/mol).

3.2 Unimolecular reactivity of alkyloxalate ions

In Table 4, the MI and CA spectra of the alkyloxalate ions are summarized. The alkyloxalate anions **1** to **5** show a rather similar behavior. Quite surprisingly, all spectra are largely dominated by a signal corresponding to the loss of neutral CO (Δm = 28). Two minor signals refer to elimination of CO_2 (Δm = 44) and to the combined loss of CO_2 and CO (Δm = 72). The spectra are thus exclusively composed by signals corresponding to CO_x losses (x = 1, 2) and no other eliminations able to compete with these processes are observed. Furthermore, almost no drastic changes are associated when the internal energy of the system is increased (CA experiment), in contrast to what is in general expected in comparing MI and CA processes [19].

Table 4

Intensities[a] of fragments in MI and CA spectra of mass-selected alkyloxalates $ROCOCOO^-$ (R = H, CH_3, C_2H_5, *i*-C_3H_7, and *t*-C_4H_9).

R (*m/z*)[b]		– CO	– CO_2	– (CO + CO_2)
1: H (89)	MI	100	1	1
	CA	100	2	2
2: CH_3 (103)	MI	100	1	1
	CA	100	1	2
3: C_2H_5 (117)	MI	100	1	1
	CA	100	2	1
4: *i*-C_3H_7 (131)	MI	100	3	1
	CA	100	3	2
5: *t*-C_4H_9 (145)	MI	100	13	0
	CA	100	16	4

[a] Intensity relative to the base peak (= 100); peaks < 1 are neglected.

[b] Mass-to-charge ratio of precursor anion in amu.

The decomposition process corresponding to the combined loss of CO_2 and CO could consist of either a direct or a consecutive loss of the neutral molecules. As only small changes in intensity for this signal are observed between the MI and CA experiments, the second hypothesis seems less likely as an internal energy gain (by collision) of the system should accordingly lead to a higher intensity. While we attribute this reaction to the formation of CO and CO_2, it has to be mentioned that, in principle, it could also correspond to the loss of a genuine neutral C_2O_3 unit. This molecule has already been extensively studied by both experiment and theory [20-25]. Peppe *et al.*[22] have shown that the most stable structure of neutral C_2O_3, in the singlet multiplicity, corresponds to a van der Waals complex (Scheme 5) which is stable with respect to dissociation to CO_2 and CO by only 1.2 kcal/mol (CCSD(T)/aug-cc-pVDZ//B3LYP/6-31G(d) level of theory). For this reason, we assume that if the neutral species with Δm = 72 correspond to C_2O_3, it seems very likely that it dissociates immediately into CO and CO_2. In the following, we will therefore assume that the mass difference of Δm = 72 corresponds to the combined formation of CO + CO_2, rather than genuine C_2O_3 [26].

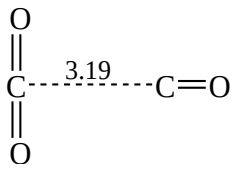

Scheme 5: Structure of most stable isomer of $^1C_2O_3$. The bond length (in Å) is taken from Peppe *et al.* [22].

The structure of the product ion and the mechanism by which decarbonylation (Δm = 28) occurs is not obvious because this fragment cannot be formed in a direct bond cleavage of the anions, as is the case for the decarboxylation or the combined elimination of CO_2 and CO. Nevertheless, the nature of the product ions due to CO loss can be easily probed by MS/MS experiments because their intensities are high enough to allow consecutive mass selection of the alkyloxalates and of the subsequently formed fragment ions.

Table 5

Intensities[a] of observed fragments[b] in the CA/CA spectra of RCO_3^- ions formed from mass-selected alkyloxalates $ROCOCO_2^-$.

R	Selection[b,c]	*m/z*[b] (Intensity[a])
H	89/61	17 (100), 60 (80)
CH_3	103/75	31 (100), 45 (48), 60 (20)
C_2H_5	117/89	43 (6), 45 (100), 60 (5)
i-C_3H_7	131/103	57 (4), 59 (100), 60 (2)
t-C_4H_9	145/117	57 (20), 60 (11), 73 (100)

[a] Intensity relative to the base peak (= 100).

[b] Mass-to-charge ratio in amu.

[c] The experiment consists in selecting the precursor ion alkyloxalates with B1 and the resulting charged fragments with E1 while B2 is scanned. The masses indicated correspond to the mass of the alkyloxalate parents and to the mass of the fragment selected with E1.

The loss of CO from the alkyloxalates formally leads to RCO_3^- ions with R = H, CH_3, C_2H_5, *i*-C_3H_7, and *t*-C_4H_9. The CA/CA mass spectra of these ions (Table 5) are dominated by signals of the corresponding alkoxide ions RO^- (loss of neutral CO_2). A characteristic peak for the loss of alkyl radicals concomitant with the generation of the radical anion $CO_3^{\bullet -}$ (*m/z* =

60) is also present, which indicates that all three oxygen atoms are bound to the same carbon atom. Moreover, in the case of the $CH_3CO_3^-$ ion, elimination of formaldehyde concomitant with formation of HCO_2^- also takes place. This CA/CA spectrum agrees thus well with the CA spectrum of methylcarbonate given by Hayes and coworkers [27], as well as the other CA/CA data given in Table 5, with CA experiments of genuine alkylcarbonate ions $ROCOO^-$ [28,29]. O'Hair and coworkers [30] have also investigated the unimolecular reactivity of $HOCOCOO^-$ ions and observed a fragment at *m/z* = 61 which they attributed to the hydrogencarbonate ion $HOCOO^-$. Consideration of the thermochemistry of the dissociation of the alkyloxalates **1-5** further reveals that the decomposition of alkyloxalate ions into alkylcarbonates and CO is quite favorable, endothermic by only few kcal/mol (Table 6). In comparison, the direct bond cleavages leading to decarboxylation as well as decarboxylation combined with decarbonylation are more than 30 kcal/mol higher in energy. Decarboxylation leads to alkoxycarbonyl anions $ROCO^-$ which are well-known species in the gas phase [31,32], and alkoxy anions RO^- are obtained by simultaneous loss of CO_2 and CO from alkyloxalates [31,33].

Table 6

Calculated heats of reaction[a] at 298 K of the observed dissociation processes of alkyloxalates **1** to **5** at the MP2/6-311++G(3df,3pd)//MP2/6-311++G(d) level of theory.

	$ROCOO^- + CO$	$ROCO^- + CO_2$	$RO^- + CO + CO_2$
1	17.7	44.9	60.3
2	9.2	35.5	47.0
3	8.7	34.2	43.8
4	5.1	32.5	38.5
5	7.4	31.3	37.6

[a] ZPE included and scaled (0.9496).

The general dissociation scheme of alkyloxylates can accordingly be summarized by three competing pathways with decarbonylation as the by far major route (Scheme 6).

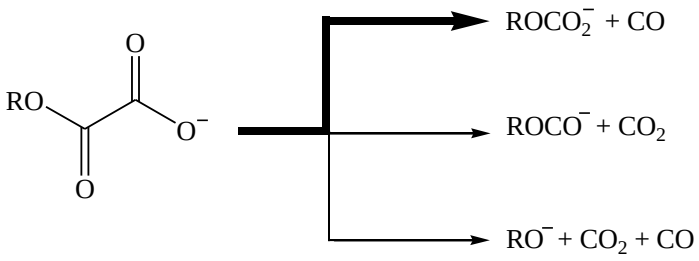

Scheme 6: General dissociation scheme of alkyloxalates ROCOCOO$^-$ for R = H, CH_3, C_2H_5, *i*-C_3H_7, and *t*-C_4H_9. The bold arrow indicates the main dissociation pathway.

As far as the direct bond cleavages are concerned, the question of mechanisms is not a burning one. In contrast, decarbonylation of alkyloxalates cannot be understood that easily because it requires a rearrangement of the anion; moreover, alkyloxylates possess two different carbonyl groups, which can possibly be eliminated. Two mechanisms appear most plausible (Scheme 7). The first one, denoted as **A**, consists in the formation of an ion-neutral complex [ROCO$^-$ CO_2] [34] from the alkyloxalate, followed by an intracomplex attack of carbon dioxide by the nucleophilic oxygen atom $O_{(4)}$ in the complex (INC_A); we note in passing that a scan of the potential energy surface revealed that the formation of INC_A proceeds without a barrier. This mechanism has been proposed by O'Hair and coworkers [30] in the study of dissociation of the hydrogen oxalate ion, but has not been probed any further neither theoretically nor experimentally. The second variant, denoted as **B**, consists in a direct attack of the electrophilic atom $C_{(2)}$ by the oxygen atom $O_{(1)}$ carrying the negative charge in alkyloxalate with subsequent elimination of CO. For acid-catalyzed decarbonylation of α-keto carbonic acid involving the carboxyl CO group, see ref. [35,36]. Experimentally, these two mechanisms could be probed by means of labeling experiments because the atoms involved are not the same [37]; however a selective synthesis of labeled ions such as ROCO^{18}COO$^-$, ROC^{13}OCOO$^-$, ROCOCOO^{18-} or ROCOC^{13}OO$^-$ is far from being trivial and was hence not pursued any further.

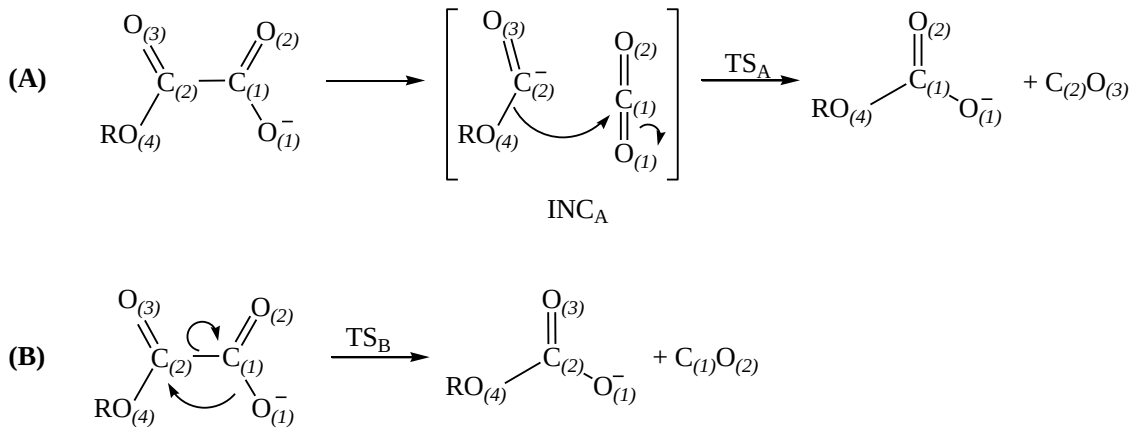

Scheme 7: Two mechanistic variants for the decarbonylation of alkyloxalates $ROCOCOO^-$ (R = H, CH_3, C_3H_5, *i*-C_3H_7, and *t*-C_4H_9).

Instead, the two mechanisms have been probed computationally. Structures and energies of the transition structures of variants **A** and **B** have been calculated at the MP2/6-311++G(3df,3pd)//MP2/6-311++G(d) level of theory, as well as the ion-neutral complex involved in mechanism **A** for the five alkyloxalates **1** to **5**. The resulting energies are summarized in Table 7.

In general, the transition structures TS_A associated with mechanism **A** are by up to 20 kcal/mol lower in energy than the TS_B related to mechanism **B**. Formation of the ion-neutral complex INC_A costs on average 30 kcal/mol relative to the alkyloxalates, except for the hydrogen oxalate ion which is 38 kcal/mol less stable. From an energetic point of view, mechanism **A** is thus much more favorable than variant **B**. What can further help to dismiss mechanism **B** is a consideration of the relative intensities of the fragment ions in the MI and CA experiments performed on alkyloxalates (Table 4) as well as the energy demands of the various fragments (Table 6). Decarbonylation dominates all spectra, what has been in part explained by a most favorable thermochemistry of the products obtained as compared to those obtained from decarboxylation and simultaneous decarboxylation and decarbonylation. Nevertheless, this dissociation requires the passage through a transition structure, whereas the two other dissociations pathways are direct bond cleavages which, most likely, require no excess activation energies. Thus, if the transition structure associated with decarbonylation were energetically extremely demanding, the alkyloxalate ions would not be able to cross it particularly in the MI process and the other dissociation pathways would be accordingly more present. Therefore, the transition structures TS_A which are similar in energy to the resulting products seems to be highly favored in the course of dissociation of alkyloxalates. By

comparing the experimental results with the energies predicted for TS_A and TS_B, we conclude that decarbonylation occurs through a mechanism of type **A**. The optimized structures of both INC_A and TS_A and of are presented in Figure 5 for each alkylcarbonates **1** to **5**.

Table 7

Total and relative energies of the transition states TS_A[a] and TS_B[a] and of the ion-neutral complex, INC_A,[a] involved in the course of decarbonylation of alkyloxalates $ROCOCOO^-$ at the MP2/6-311++G(3df,3pd)//MP2/6-311++G(d) level of theory.

		E_{tot}[b] (Hartree)	E_{rel}[c] (kcal/mol)
	TS_A	-377.1428343	43.7
1: H	INC_A	-377.1513545	38.3
	TS_B	-377.1044195	67.8
	TS_A	-416.3154505	36.3
2: CH_3	INC_A	-416.3239468	30.9
	TS_B	-416.2786243	59.4
	TS_A	-455.5148716	36.1
3: C_2H_5	INC_A	-455.5234566	30.7
	TS_B	-455.477117	59.7
	TS_A	-494.716657	33.6
4: *i*-C_3H_7	INC_A	-494.725741	27.9
	TS_B	-494.657488	70.7
	TS_A	-533.9136187	37.7
5: *t*-C_4H_9	INC_A	-533.9236912	31.4
	TS_B	-533.877084	60.6

[a] TS_A and TS_B correspond to the respective transition structures associated with the mechanistic variants **A** and **B** (Scheme 7), and INC_A stands for the ion-neutral complex formed prior to decarbonylation.

[b] ZPE included and uniformly scaled (0.9496).

[c] Energies are given relative to those of the alkyloxalates (Table 2) in their most stable conformation.

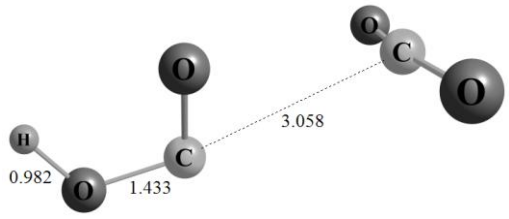

INC_A(**1**)

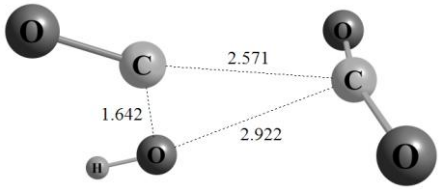

TS_A(**1**)

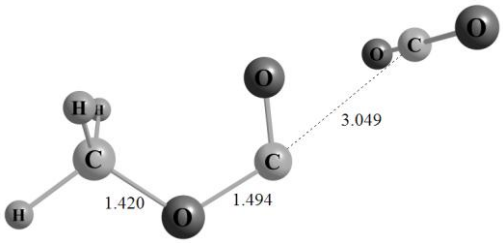

INC_A(**2**)

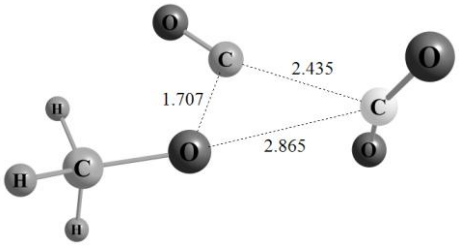

TS_A(**2**)

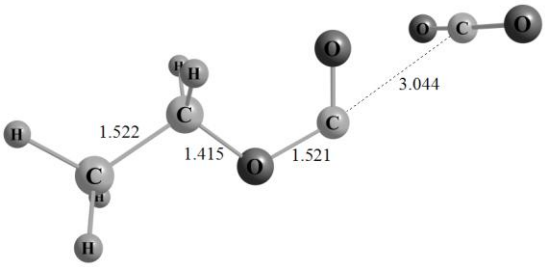

INC_A(**3**)

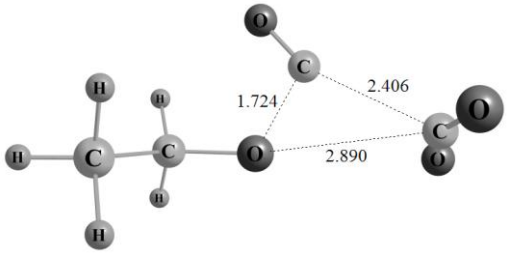

TS_A(**3**)

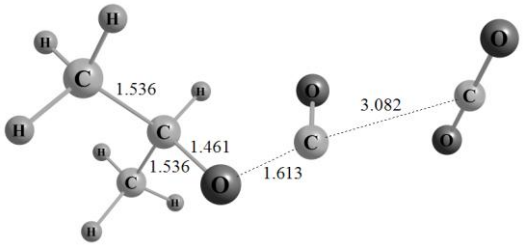

INC_A(**4**)

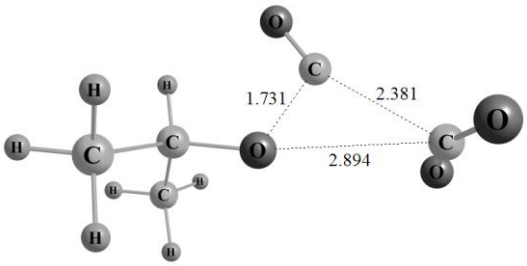

TS_A(**4**)

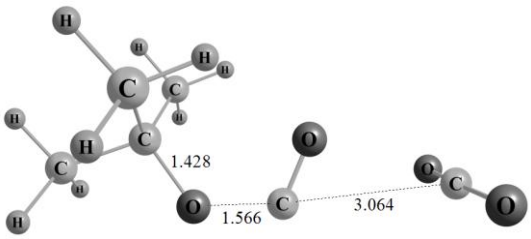

INC_A(**5**)

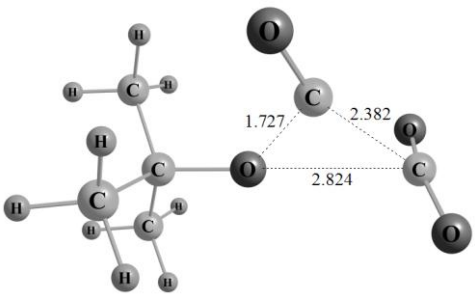

TS_A(**5**)

Figure 5: Optimized structures of the ion-neutral complexes INC_A and the transition structures TS_A for the five alkyloxalates under study at the MP2/6-311++G(d) level of theory.

4. Conclusions

The different conformers of alkyloxalates $ROCOCOO^-$ are investigated computationally for R = H, CH_3, C_2H_5, *i*-C_3H_7, and *t*-C_4H_9. The results show that the most stable conformers differ according to the substituent R; due an intramolecular hydrogen bond, the hydrogen oxalate ion **1** is most stabilized in a planar *cC* conformation, whereas a trans (*T*) conformation between the two carbonyl groups is preferred for the larger substituents. The favorable spatial position of the substituents also differs with R. The most stable conformation with respect to rotation around the $O_{(4)}$–$C_{(2)}$ bond is cis for R = H, CH_3, and C_2H_5, whereas the trans conformation is favored for R = *i*-C_3H_7 and *t*-C_4H_9. Further, alkyloxalates anions have been submitted to MI and CA experiments in order to investigate their unimolecular and their collision-induced dissociation behavior. The results are similar for all substituents and three decomposition pathways are observed: decarbonylation, decarboxylation, and simultaneous decarboxylation and decarbonylation. The first pathway is by far the dominant decomposition process observed in both MI and CA experiments, which is also confirmed from a thermochemical point of view. Loss of CO leads to the formation of alkylcarbonates $ROCOO^-$, whereas elimination of CO_2 leads to alkoxycarbonyl anions $ROCO^-$, and the combined production of CO and CO_2 affords the corresponding alkoxy anions RO^-. While the two latter decomposition paths correspond to direct bond cleavages, decarbonylation requires a rearrangement of the anions which is suggested to proceed via the formation of an intermediate ion-neutral complex.

Acknowledgements

This work was supported by the Deutsche Forschungsgemeinschaft and the Fonds der Chemischen Industrie. We thank the Institut für Mathematik of the Technische Universität Berlin and the Norddeutscher Verbund für Hoch- und Höchstleistungsrechnen (HLRN) for the generous allocation of computer time.

References

[1] J.H. Bowie, Mass Spec. Rev. 9 (1990) 349.
[2] C.A. Schalley, D. Schröder and H. Schwarz, Int. J. Mass Spectrom. Ion Processes 153 (1996) 173.
[3] W.J. Richter and H. Schwarz, Angew. Chem., Int. Ed. Engl. 17 (1978) 424.
[4] Y.L. Guo and J. Grabowski, Int. J. Mass Spectrom. Ion Processes 117 (1992) 299.
[5] D. Schröder, H. Soldi-Lose and H. Schwarz, Aust. J. Chem. 56 (2003) 443.
[6] C. Møller and M.S. Plesset, Phys. Rev. 46 (1934) 618.
[7] T. Clark, J. Chandrasekhar, G.W. Spitznagel and P.v.R. Schleyer, J. Comput. Chem. 4 (1983) 294.
[8] R. Krishnan, J.S. Binkley, R. Seeger and J.A. Pople, J. Chem. Phys. 72 (1980) 650.
[9] M.J. Frisch, G.W. Trucks, H.B. Schlegel, G.E. Scuseria, M.A. Robb, J.R. Cheeseman, J. Montgomery, J.A., T. Vreven, K.N. Kudin, J.C. Burant, J.M. Millam, S.S. Iyengar, J. Tomasi, V. Barone, B. Mennucci, M. Cossi, G. Scalmani, N. Rega, G.A. Petersson, H. Nakatsuji, M. Hada, M. Ehara, K. Toyota, R. Fukuda, J. Hasegawa, M. Ishida, T. Nakajima, Y. Honda, O. Kitao, H. Nakai, M. Klene, X. Li, J.E. Knox, H.P. Hratchian, J.B. Cross, V. Bakken, C. Adamo, J. Jaramillo, R. Gomperts, R.E. Stratmann, O. Yazyev, A.J. Austin, R. Cammi, C. Pomelli, J.W. Ochterski, P.Y. Ayala, K. Morokuma, G.A. Voth, P. Salvador, J.J. Dannenberg, V.G. Zakrzewski, S. Dapprich, A.D. Daniels, M.C. Strain, O. Farkas, D.K. Malick, A.D. Rabuck, K. Raghavachari, J.B. Foresman, J.V. Ortiz, Q. Cui, A.G. Baboul, S. Clifford, J. Cioslowski, B.B. Stefanov, G. Liu, A. Liashenko, P. Piskorz, I. Komaromi, R.L. Martin, D.J. Fox, T. Keith, M.A. Al-Laham, C.Y. Peng, A. Nanayakkara, M. Challacombe, P.M.W. Gill, B. Johnson, W. Chen, M.W. Wong, C. Gonzalez and J.A. Pople. GAUSSIAN 03, Revision C.02, 2004.
[10] A.P. Scott and L. Radom, J. Phys. Chem. 100 (1996) 16502.
[11] M.J. Frisch, J.A. Pople and J.S. Binkley, J. Chem. Phys. 80 (1984) 3269.
[12] C.W. Bock and R.L. Redington, J. Chem. Phys. 85 (1986) 5391.
[13] J. Higgins, X. Zhou, R. Liu and T.T.S. Huang, J. Phys. Chem. A 101 (1997) 2702.
[14] A. Mohajeri and N. Shakerin, J. Mol. Struct. 711 (2004) 167.
[15] M. Remko, K.R. Liedl and B.M. Rode, J. Chem. Soc., Perkin Trans. 2 (1996) 1743.
[16] J. Tyrrell, J. Mol. Struct. (THEOCHEM) 258 (1992) 389.
[17] C. Van Alsenoy, V.J. Klimkowski and L. Schafer, J. Mol. Struct. (THEOCHEM) 109 (1984) 321.
[18] C. Cheng and S.-F. Shyu, Int. J. Quantum Chem. 76 (2000) 541.
[19] K. Levsen and H. Schwarz, Mass Spec. Rev. 2 (1983) 77.
[20] J. Langlet, J. Caillet, M. Allavena, V. Raducu, B. Gauthier-Roy, R. Dahoo and L. Abouaf-Marguin, J. Mol. Struct. 484 (1999) 145.
[21] J.S. Muenter and R. Bhattacharjee, J. Mol. Spectrosc. 190 (1998) 290.
[22] S. Peppe, S. Dua and J.H. Bowie, J. Phys. Chem. A 105 (2001) 10139.
[23] R.W. Randall, J.P.L. Summersgill and B.J. Howard, J. Chem. Soc., Faraday Trans. 86 (1990) 1943.
[24] Y. Xu, A.R.W. McKellar and B.J. Howard, J. Mol. Spectrosc. 179 (1996) 345.
[25] V. Raducu, B. Gauthierroy, R. Dahoo, L. Abouafmarguin, J. Langlet, J. Caillet and M. Allavena, J. Chem. Phys. 102 (1995) 9235.
[26] D. Schröder, H. Schwarz, S. Dua, S.J. Blanksby and J.H. Bowie, Int. J. Mass Spectrom. 188 (1999) 17.

[27] R.N. Hayes, R.J. Waugh and J.H. Bowie, Rapid Commun. Mass Spectrom. 3 (1989) 338.
[28] P.C.H. Eichinger and J.H. Bowie, Int. J. Mass Spectrom. Ion Processes 123 (1991) 110.
[29] H. Soldi-Lose, D. Schröder and H. Schwarz, Int. J. Mass Spectrom. (2007) to be submitted.
[30] R.A.J. O'Hair, J.H. Bowie and R.N. Hayes, Rapid Commun. Mass Spectrom. 2 (1988) 275.
[31] S.T. Graul and R.R. Squires, J. Am. Chem. Soc. 110 (1988) 607.
[32] D. Schröder, M. Semialjac and H. Schwarz, Eur. J. Mass Spectrom. 9 (2003) 287.
[33] T.M. Ramond, G.E. Davico, R.L. Schwartz and W.C. Lineberger, J. Chem. Phys. 112 (2000) 1158.
[34] N. Heinrich and H. Schwarz, in "Ion and Cluster-Ion Spectroscopy and Structure", J. P. Maier (Ed.), Elsevier, Amsterdam (1989) p. 329.
[35] K. Banholzer and H. Schmid, Helv. Chim. Acta 39 (1956) 548.
[36] W.W. Elliott and D.L. Hammick, J. Chem. Soc. (1951) 3402.
[37] P.C.H. Eichinger, R.N. Hayes and J.H. Bowie, J. Chem. Soc., Perkin Trans. 2 (1990) 1815.